Final Technical Report on:

INFLUENCE OF A MAGNETIC FIELD DURING DIRECTIONAL SOLIDIFICATION OF MAR-M 246 + Hf SUPERALLOY

Submitted by

J. Barry Andrews
Department of Materials Science & Engineering
University of Alabama at Birmingham
Birmingham, Alabama 35294

and

Wendy Alter, Dianne Schmidt
Materials and Processes Laboratory
NASA/George C. Marshall Space Flight Center
Marshall Space Flight Center, Alabama 35812

for

NASA Contract NAS8-36461
George C. Marshall Space Flight Center
Marshall Space Flight Center, Alabama 35812

January, 1991

Final Technical Report on:

INFLUENCE OF A MAGNETIC FIELD DURING DIRECTIONAL SOLIDIFICATION OF MAR-M 246 + Hf SUPERALLOY

Submitted by

J. Barry Andrews
Department of Materials Science & Engineering
University of Alabama at Birmingham
Birmingham, Alabama 35294

and

Wendy Alter, Dianne Schmidt
Materials and Processes Laboratory
NASA/George C. Marshall Space Flight Center
Marshall Space Flight Center, Alabama 35812

for

NASA Contract NAS8-36461
George C. Marshall Space Flight Center
Marshall Space Flight Center, Alabama 35812

January, 1991

TABLE OF CONTENTS

ABSTRACT

An area that has been almost totally overlooked in the optimization of properties in directionally-solidified superalloys is the control of microstructural features through the application of a magnetic field during solidification. This project was designed to investigate the influence of a magnetic field on the microstructural features of a nickel-base superalloy. Studies were carried out on the dendritic MAR-M 246+Hf alloy, which was solidified under both a 5K gauss magnetic field and under no-applied-field conditions. The possible influences of the magnetic field on the solidification process were observed by studying variations in microstructural features including volume fraction, surface area, number and shape of the carbide particles. Stereological factors analyzed also included primary and secondary dendrite arm spacing and the volume fraction of the interdendritic eutectic constituent. Microprobe analysis was carried out to determine the chemistry of the carbides, dendrites and interdendritic constituent, and how it varied between field and no-field solidified samples. Experiments involving periodic application and removal of the magnetic field were also performed in order to permit a comparison with structural variations observed in a MAR-M 246+Hf alloy solidified during KC-135 high-g, low-g maneuvers.

INTRODUCTION

One of the major goals in the area of solidification research today is the control of microstructural features in order to produce components that exhibit outstanding properties. Proper control is of particular importance in the production of sophisticated superalloy parts by directional solidification processes. However, control of microstructures to date has been primarily limited to modification of alloy composition and to variations in thermal gradients and solidification rates during solidification. A recent investigation has shown that directional solidification under low gravity conditions can lead to changes in the dendrite arm spacing, the volume fraction of carbides formed, and the amount of interdendritic segregation in superalloys. It is likely that solidification under other conditions that reduce fluid flow in advance of the solid-liquid interface can alter microstructures as well. One possibility of inhibiting this fluid flow is through solidification under a magnetic field.

A major limitation in obtaining desirable microstructures in superalloys is the difficulty in controlling the solidification process in such a way that several microstructural features can be optimized. It is well known that the degree of segregation, the dendrite arm spacing, the amount of interdendritic phase, and the carbide volume fraction, distribution and morphology all influence the mechanical properties of advanced Ni-based superalloys[2]. The benefits that can be gained through control of microstructural

features, particularly carbide volume fraction, shape and distribution, is expected to be significant. However, control of all of these features during solidification is not currently feasible.

One serious hinderance to understanding microstructural evolution during directional solidification has been the inability to impede gravitational and non-gravitational driven flows.[3] Studies performed as early as 1966 indicated that fluid flow could essentially be stopped by solidification under a magnetic field.[4] Performance of solidification experiments under the influence of a magnetic field can dampen both gravitational and non-gravitational driven flows. It is hoped that the increased level of understanding of the solidification process obtained from these experiments may eventually lead to the ability to produce microstructures of desired morphologies.

The purpose of this research program was to investigate the influence of a magnetic field on the microstructural features obtained during directional solidification of the dendritic superalloy, MAR-M 246+Hf. Testing was carried out using both steady magnetic field and alternating field conditions.

MICROSTRUCTURE-PROPERTY RELATIONSHIPS IN SUPERALLOYS

It is well known that variations in the thermal gradients and solidification rates during directional solidification can lead to changes in the microstructural features of the alloy solidified.[5] These microstructural changes can have a significant influence on the properties of the alloy. In superalloys, the principal microstructural variables include:

1. the carbide amount and morphology
2. the amount of the interdendritic constituent
3. the primary and secondary dendrite spacing.

Microstructural control is achieved through composition selection or modification as well as through the control of processing variables.

The influence of some microstructural features on alloy properties has not been rigorously determined. One area in which this is the case is the influence of carbide morphology and distribution on the properties of certain nickel-base superalloys.[2] This includes the MAR-M 246+Hf alloy currently in use in the Space Shuttle Main Engine (SSME) turbopumps. Either script or blocky carbide morphologies can be obtained in this alloy. Surprisingly, there is no clear cut answer as to which form is preferable in particular applications.

In general, the advanced nickel-base superalloys, such as the MAR-M 246+Hf, contain substantial levels of aluminum and titanium which strengthen the austenitic matrix through precipitation of

$Ni_3(Al,Ti)$, an ordered, FCC compound referred to as "gamma prime" (γ').[6] The carbides MC, $M_{23}C_6$, and M_6C provide limited matrix strengthening through dispersion hardening. However, their dominate role is stabilization of grain boundaries against excessive shear.[2]

Carbides can exert a profound influence on properties by their precipitation on grain boundaries.[2] The distribution of carbides in cast superalloys can be marginally modified by heat treatment. However, true solutionizing, in which all minor constituents are dissolved, is not considered feasible in most nickel-base superalloys since the MC carbides usually will not totally dissolve without incipient melting of the alloy.

Matrix and grain boundary carbides can have a negative influence on alloy mechanical properties.[2] Oxidized carbides or precracked carbides from machining or thermal stresses can initiate fatigue cracks. Both carbide size and shape is important. Reduced carbide volume fractions and sizes result in a reduction of precracked carbides. In addition, it is generally assumed that carbides of a script morphology are more likely to lead to fatigue crack formation than blocky carbides. However, testing of this latter assumption is difficult because it is almost impossible to obtain samples in which the only microstructural variation is carbide morphology. A variation in solidification rate can lead to changes in carbide morphology under some circumstances, for example, from a blocky to a script type structure. However, variations in dendrite arm spacing and other microstructural

features usually occur at the same time, making determination of the influence of carbide morphology alone difficult.

Directional solidification under low-gravity conditions has been shown to influence microstrucural features considerably.[1] It is expected that solidification under a magnetic field will severely restrict the movement of fluid in advance of the solidification front and result in a significant microstructural change as well. Through proper control of the solidification process and magnetic field, it may be possible to produce alloys with controlled microstructural features.

SOLIDIFICATION UNDER A MAGNETIC FIELD

The influence of a magnetic field on the solidification process has been studied for well over two decades. From the earliest studies[4] it has been apparent that the major influence of a magnetic field during solidification is one of restricting fluid movement. Thermal convection in electrically conducting fluids is inhibited by the application of a magnetic field, since motion of the conducting fluid across magnetic field lines is subject to inductive drag.[4] The primary effect is one of apparent increased liquid metal viscosity in the presence of the field. This is a useful concept for analyzing some of the more straight forward circumstances encountered. Unfortunately, the solidification process, particularly when convection due to both thermal and compositional gradients is involved, is complex problem.[7] In

addition, a magnetic field may influence the solidification process in other ways than just restricting fluid flow.

While increased apparent viscosity is an easily grasped concept, it does not completely describe the actual influence of a magnetic field. For example, early theoretical investigations treating the influence of a magnetic field on thermal convection in a conducting fluid indicated that field orientation relative to the gravitational vector should be of importance.[8,9] It has been suggested that the magnetic field should be oriented parallel to the gravitational vector if convection is to be most effectively suppressed.

There is no question that magnetic fields can have a considerable influence on the solidification process. The few studies that have been carried out have shown this. However, the reported changes resulting from the presence of the field have been somewhat inconsistent. Although some microstructural modification is expected, no quantitative microstructural parameters have been reported. It is essential that an indepth study be carried out to determine the influence of a magnetic field on the microstructures developed. For superalloys, although many of the microstructures obtained are complex, quantitative microscopy methods exist for characterizing most of the microstructural parameters of importance. The following sections cover the findings that have been reported to date concerning the influence of a magnetic field on the solidification process. The literature search revealed no studies involving superalloy systems.

The Influence of a Magnetic Field on Solute Banding

Directional solidification of alloys, particularly when horizontal growth directions are utilized, often leads to solute banding. Most of the early studies involving solidification in the presence of a magnetic field were concerned with the elimination of this solute banding in horizontally solidified samples.[10,11] The banding, which resulted from turbulent convection currents, was found to be effectively eliminated with the application of a vertically oriented magnetic field. Later studies which investigated the magnetic flux densities required to suppress convection in molten tin, indicated that for a horizontal temperature gradient of 10°C/cm, a flux density of approximately 500 Gauss was sufficient to prevent turbulent convection.[4] However, laminar convection was found to continue until flux densities approaching 2000 Gauss were applied. It was also noted that the horizontal temperature gradient in advance of the solidification front was substantially increased in the presence of the magnetic field; presumably because of a significant reduction in the convective mode of heat transfer.

In 1980, Coriell, et al. carried out a study concerned primarily with modeling convective and interfacial instability criteria during directional solidification. It was indicated in this analysis that a vertical magnetic field would increase the critical concentration required for convective instabilities.For the system analyzed (Pb-Sn), a field of 10,000 Gauss was needed to

cause an order of magnitude change in the critical concentration. While high field strengths may be necessary, this work did indicate that a magnetic field could actually prevent the onset of convection.

The Influence of a Magnetic Field on Segregation

Several studies have indicated that solidification under a magnetic field will alter the solute distribution in a sample. For example, in 1966, Utech et al.[12] found that a vertical magnetic field of 3500 G applied to a tin - 1% bismuth sample directionally solidified in an open horizontal boat resulted in a more uniform composition profile. Work performed by Sanghamitra and Wilcox[13] in 1978 studied vertical directional solidification of an InSb -GaSb alloy with and without a horizontal magnetic field. In this work, segregation was not influenced by the presence of the magnetic field for slow growth rates and high thermal gradients. However, the composition of samples solidified at higher rates was influenced by the field. Since a greater effect was noted at the high growth rates, the authors concluded that the magnetic field was effective in reducing buoyancy driven natural convection, but did not eliminate it.

It would appear that if the primary influence of a magnetic field was to limit convection, solidification under a magnetic field would prevent disruption of the solute boundary layer and mixing in the liquid.This should result in a more uniform

longitudinal compositional profile during planar growth front conditions.

The Influence of a Magnetic Field on Microstructure

One shortcoming of the solidification process is the inability to independently control several of the more significant microstructural features of an alloy. This is particularly true in the more complex, multicomponent alloys such as superalloys. While many of these features are obviously interrelated, there are many that can theoretically be independently varied. This is particularly true in the more complex, multicomponent alloys such as superalloys. Proper control of the carbide and dendritic structures in some superalloys could have a significant influence on their properties.The application of a magnetic field gives a means of microstructural control that may make optimization of these microstructures possible.

The influence of magnetic fields on the microstructures obtained during directional solidification has been a topic of considerable interest for some time. One of the first investigations to address microstructural variations in metal systems due to the presence of a magnetic field was carried out in 1969 by Sahm.[14] The gold-cobalt eutectic system studied was somewhat specialized in that the Curie Temperature of the cobalt phase was higher than the eutectic temperature. During vertical directional solidification of eutectic and off-eutectic alloys, a

magnetic field applied parallel to the growth direction was found to coarsen the Co-phase in the fibrous composite structure. In addition, for hypereutectic alloys, an orienting effect on the primary Co-dendrites was noted due to the field. A more detailed report at a later date[15] indicated that the shape and size of the eutectic fibers was modified by the field as well. This was though to be due to a field induced enhancement of the local temperature gradient.

On the other hand, not all studies have reported significant effects due to solidification in a magnetic field. Work reported by Verhoeven and Pearson in 1973[18] stated that eutectic Sn-Cd and Sn-Pb alloys solidified vertically were not influenced by a transverse magnetic field. No effect was found on the spacing or orientation of the lamellar structure. They concluded that lamellar spacing could not be controlled by a magnetic field. It should be pointed out that directional solidification of an alloy of eutectic composition would not have resulted in the formation of a solute boundary layer. It is this boundary layer which is usually influenced by convection and would have the highest possibility of being altered by the presence of a magnetic field. As a result, Verhoven and Pearsons[18] findings are not all that surprising.

A more recent study carried out by Aoki et al.[17] involved vertical directional solidification of a hypoeutectic Al-Si alloy in a vertical magnetic field. It was found that application of the field resulted in a drastic change in the number of dendrites

present; going from many to a single large dendrite when the magnetic field was applied. Removal of the field resulted in the opposite effect. Unfortunately, in the sample processed, removal of the field also coincided with impingement of the single dendrite on the crucible wall. Aoki et al.[17] concluded that the influence of the field was to suppress dendrite formation. However, their results could be interpreted to indicate coarsening in the presence of a field as well; a finding that would be in agreement with that of Sahm[14] in 1969.

This summarizes most of the studies carried out to date concerning microstructural modification caused by the presence of a magnetic field during solidification. The reported findings show different influences of magnetic fields on microstructures among the alloy systems investigated. In some cases major changes resulted. However, no changes were found in other cases. Unfortunately, there is currently no fundamental explanation of these interesting observations and much obviously remains to be learned concerning the modification of microstructures through the use of magnetic fields.

OBJECTIVE OF THE CURRENT INVESTIGATION

In this study, a currently utilized superalloy, MAR-M 246+Hf, was solidified under both no magnetic field and magnetic field conditions in order to determine the influence of the field on microstructural features. The magnetic field applied during

solidification was expected to have a considerable influence on the microstructures obtained. Field orientation may have an effect as well. A horizontal field orientation was utilized in this investigation due to experimental restrictions. However, experiments should eventually be carried out using a field direction parallel to the gravitational vector.

These experiments quantitatively compare the microstructural features of MAR-M 246+Hf, directionally solidified with and without the influence of a magnetic field. This is a significant departure from the majority of prior solidification studies. The benefits of taking a quantitative approach will be a detailed description of the way in which microstructural features are varied through manipulation of the solidification process by the use of magnetic fields.

RESEARCH APPROACH

A MAR-M 246+Hf, nickel base superalloy was utilized in this investigation. This alloy was selected because of the vast experience of NASA personnel working with the alloy and due to the possibility of comparing the field solidification experiments with low-g, high-g solidification experiments performed during parabolic maneuvers in NASA's KC-135 zero-g aircraft.

A detailed investigation of microstructural features was carried out under a) no field conditions, b) under steady field conditions, and c) under cyclic field conditions. A vertical solidification direction was used to facilitate processing and permit a comparison of results with those obtained through solidification during alternating gravity level conditions. A horizontal magnetic field orientation was utilized.

It is common in investigations of this nature to alter conditions during the solidification experiment by varying some pertinent external parameter. This permits a determination of the influence of the variable through comparison of different regions on the same sample. For example, in the current project this could be done in order to determine the influence of a variation in solidification rate or magnetic field strength on the solidification process.

While this approach can be quite convenient, it must be realized that the structures which result due to an alteration in a parameter usually consists of a transient region followed by the

development of a region representative of steady state conditions. As an example, if the solidification rate used is suddenly increased during directional solidification under steady state, planar interface conditions, the resulting alteration in the boundary layer usually results in a solute band caused by a local increase in solute content. This is only a transient structure. However, a significant time period may elapse before steady state conditions are again established. It is well known that any comparisons made between structures obtained at different solidification rates on the same sample must be made between the structures obtained under steady state conditions.

It is reasonable to expect that the application of a magnetic field during solidification will similarly result in the formation of a transient region followed by the establishment of steady state conditions. However, the changes that result are expected to be slightly more complex than those common for solidification rate changes. For example, if the magnetic field is applied during solidification, the resulting change in magnetic flux density will induce electrical current flow in the metal. This may result in both inductive stirring and heating. The variation in magnetic flux density would be of rather short duration, but due to the field strength involved, could produce a significant change in both the flow velocity in the liquid and in the metal temperature. Once the desired field strength is reached and a non-varying field is maintained, any movement in the fluid would be damped, including the movement induced during the application of the field. While

it may appear at first glance that steady state conditions have been reached at this point, this is not actually the case. It has been shown that the presence of a magnetic field and the resulting restriction in fluid movement may lead to establishment of a new temperature profile during directional solidification due to a reduction in the convective mode of heat transfer.[4,10] Utech and Flemings[4] indicated that after application of a magnetic field, several minutes were required for local temperatures to readjust. Experimental conditions in the current investigation were designed to avoid this problem.

In order to avoid complications from these transient conditions, most samples were solidified completely under either an applied magnetic field or under no field conditions. The samples were then compared, with care being taken to compare microstructures at similar positions in the samples.

The Usefulness of Shape Factor Measurements

As discussed above, carbides which precipitate in superalloy grain boundaries can provide a strengthening function by inhibiting grain boundary sliding. While grain boundary carbides can increase the high-temperature lifetime of superalloy components, brittle intragranular carbides may also serve as crack initiation sites which can lead to fracture.

There is a lack of agreement concerning which carbide morphology is least detrimental to material properties. Some

investigators state that large blocky carbides are more prone to cracking due to their size. Other investigators suggest that script carbides may act as crack initiation sites due to their platelike shape and sharp edges. As a first step in this investigation an effort was made to characterize these two types of carbides quantitatively in order to develop a useful system for describing carbide morphologies.

Obviously, due to their geometry, script carbides are expected to have a higher surface area per unit volume than blocky carbides. However, S_v measurements cannot be used alone as an indicator of script vs. blocky carbide morphology. As an example, a structure containg many small blocky carbides and one with only a few larger convoluted carbides could have the same S_v values. The volume fraction and particle size of the carbides must be considered as well since both directly effect the total carbide surface area.

Unfortunately, the determination of mean particle size may be misleading. While these measurements are straight forward for blocky carbides which have a fairly consistant shape, script carbides are rather convoluted. Carbides which appear as discrete particles on the plane section are frequently interconnected within the matrix.

By introducing a number per area count, the distinction between large, convoluted particles and many regular particles may be clarified. While a good deal has been written on describing particle shapes[18] Fischmeister[19] has proposed a shape factor which incorporates the above measurements into a dimensionless number,

F_1, which is represented by the following equation:

$$F_1 = (2/3)\ \pi \bullet (N_L^2/V_V N_A)$$

It should be pointed out that this shape factor may be somewhat misleading. Discrete areas of carbide on the plane section are counted as individual particles. In the case of script morphology, they are probably arms of a larger carbide network. Thus the N_A count does not reflect the N_v with much accuracy, and F_1 factors provide a doubtful indication of crack propagation path length.

In order to test the usefullness of F_1, in describing carbide morphology, two samples were compared which had been processed to obtain significantly different relative amounts of blocky vs script carbides. A detailed analysis yielded no significant correlation between F_1 values and carbide morphology. As a result, the use of F_1 for determination of carbide shape is questionable. The use of this term is discussed more fully in the section covering solidification under a cyclic magnetic field.

EXPERIMENTAL PROCEDURE

Directional Solidification

The directional solidification furnace utilized is shown in Figure 1. The furnace uses a platinum wire wound core capable of reaching temperatures above 1600°C. Furnace translation is accomplished through a drive screw which is turned by a gear box

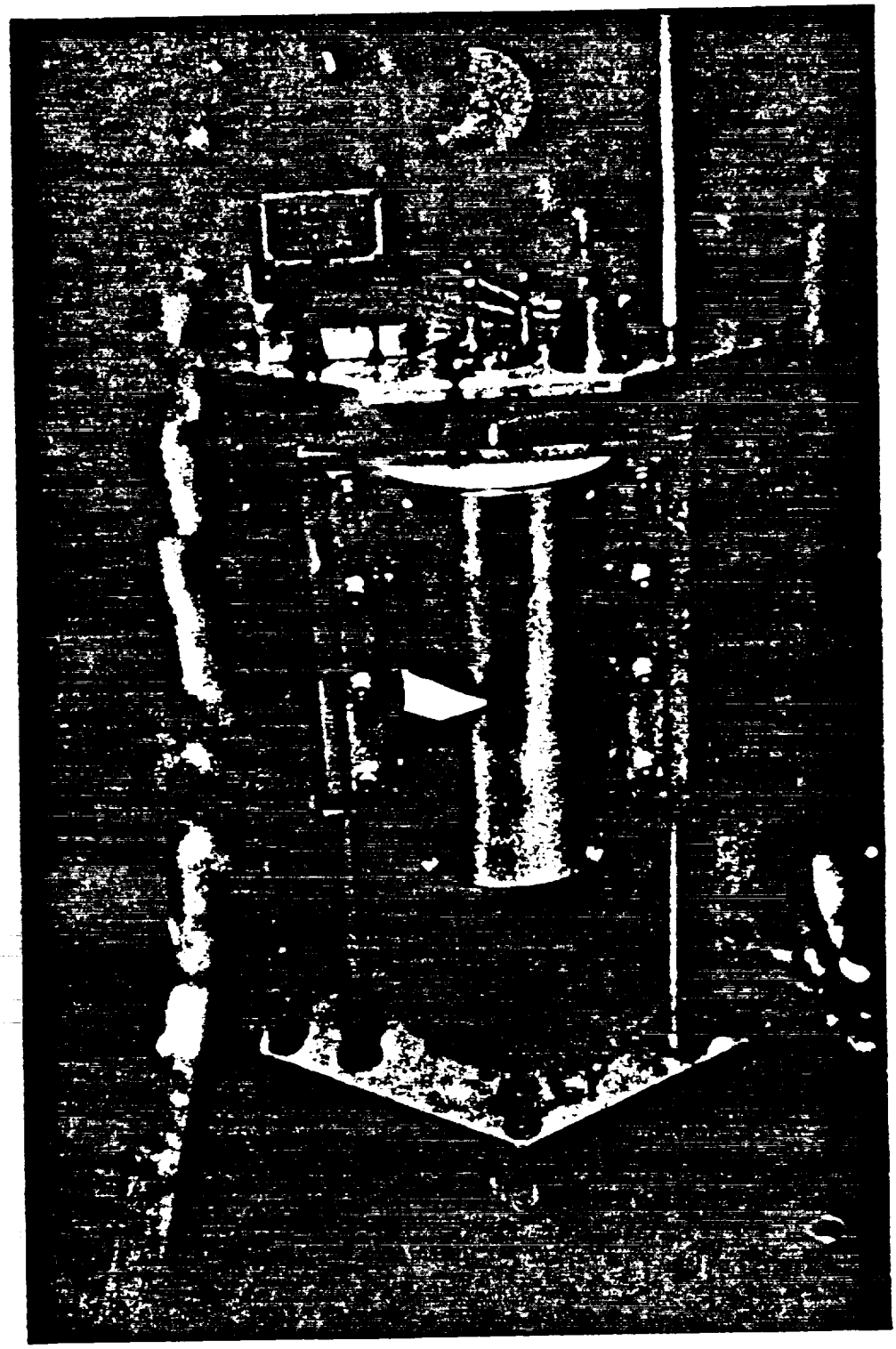

Figure 1. The directional solidification furnace utilized in the current study.

assembly and variable speed motor. Samples up to 9.5 mm in diameter can be processed in the furnace. For the current directional solidification studies, MAR-M 246 + Hf bars approximately 4 mm square in cross section were used as the starting material. Processing was carried out in 6 mm ID by 8 mm OD Al_2O_3 crucibles 46 cm in length under an argon atmosphere. The relative position between the bottom of the sample and the furnace was controlled so that the entire sample was melted before processing. Samples were held for a time period after melting in order to allow mixing to help provide a uniform liquid composition. A maximum furnace temperature of 1450°C was utilized which resulted in a temperature gradient of approximately 70°C/cm at the liquidus and 135°C/cm at the solidus.

A furnace translation rate of 1 cm/min was utilized for all directional solidification runs in this investigation. "No-field" samples were solidified with the furnace assembly between the magnet pole pieces as shown in Figure 2 but no field was applied. The entire sample was solidified at the same furnace translation rate.

Magnetic field solidification runs were carried out under a nominal applied magnetic field of 5,000 Gauss. The field uniformity was measured with a magnetometer placed in the bore of the cold furnace assembly and is shown in Figure 3.

Notice that a relatively uniform field intensity is only obtained over a 5 cm region near the center of the pole pieces. This limits the usable sample length to approximately 5 cm. When

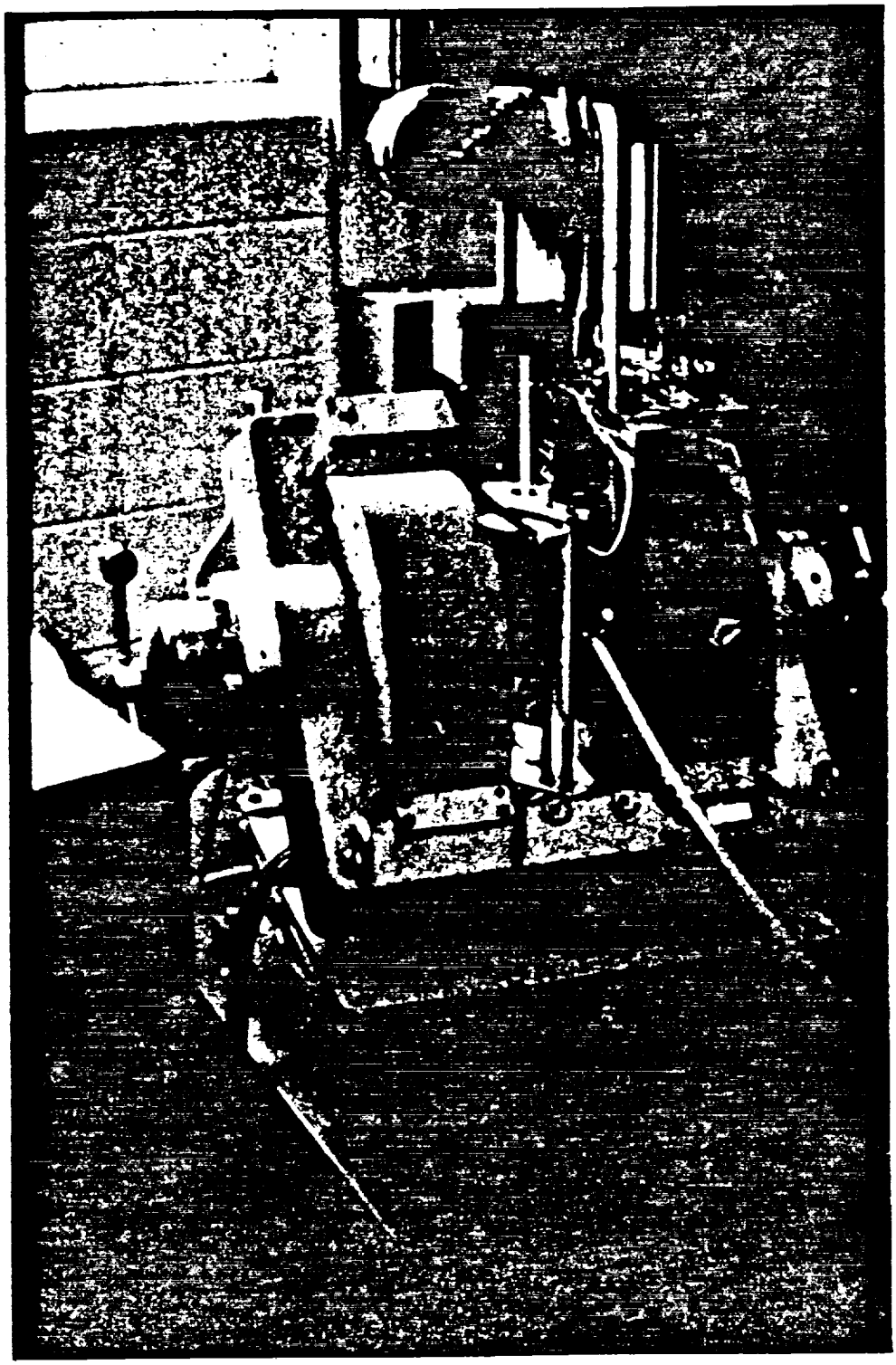

Figure 2. Furnace shown mounted between the pole pieces of the magnet.

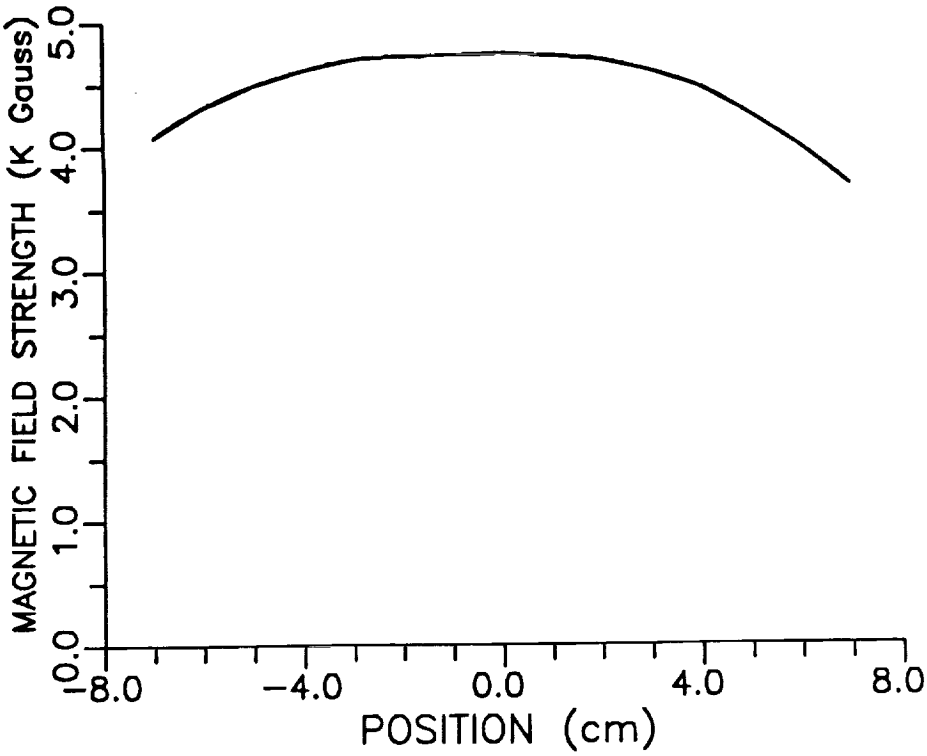

Figure 3. Magnetic field strength as a function of position for the magnet utilized in the current study. The center line of the pole pieces is defined as the zero position.

processing samples in a magnetic field, the furnace and sample were positioned so that the bottom of the sample was at the lower edge of the uniform field strength region. The furnace was held stationary while the sample was melted with no magnetic field applied and left stationary for a time period after the desired region was molten to homogenization of the melt. The magnetic field was then applied and allowed to stabilize for several minutes. The furnace was then translated up the sample at a uniform rate with the field applied. In most cases, the growth rate and field strength were held constant until the entire sample was solidified.

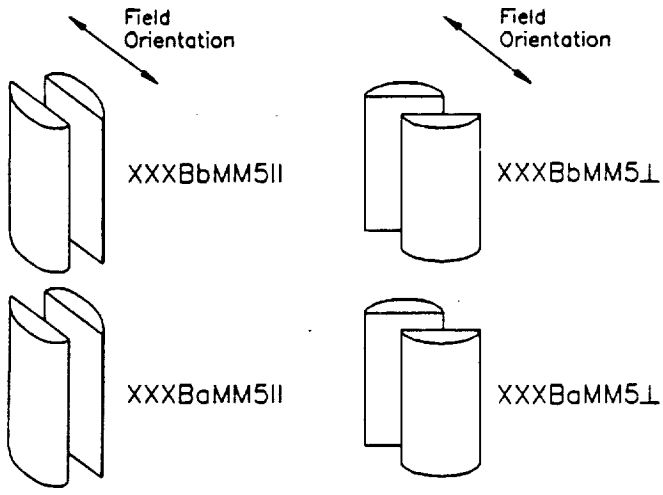

Figure 4. Sectioning scheme used for samples processed during the later stages of the project.

Analysis

After solidification, the samples were longitudinally sectioned and prepared for metallographic analysis. The first magnetic field solidified samples were sectioned in a direction parallel to the magnetic field lines. During the later stages of the project several samples were sectioned perpendicular to the magnetic field lines as well. The sectioning scheme utilized is shown in Figure 4. The numbering scheme is explained in Figure 5. The first set of measurements were taken over a section 3 cm in length with measurements at every 0.5 cm. Measurements were also taken at different radial positions including the center of the sample and 2 mm in from each edge. Parameters measured included volume fraction of the carbides, and secondary dendrite arm

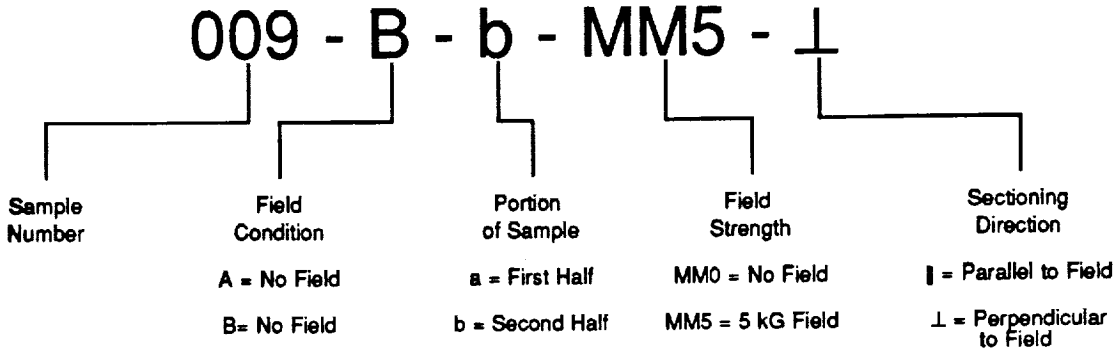

Figure 5. Sample numbering scheme.

spacing. Compositional analysis was carried out along with the volume fraction of the interdendritic structure (eutectic) and the primary dendrite arm spacing.

RESULTS AND DISCUSSION

The presence of a magnetic field and the elimination of convective flows is expected to lead to modification of the compositional and temperature gradients in advance of the solidification front. These modifications can lead to a resulting change in microstructure. This portion of the study was carried out in order to observe the microstructural changes brought about by the presence of a 5K Gauss magnetic field during directional solidification. The samples processed along with the conditions utilized are listed in Table 1.

Table 1. Sample Identification Numbers and Processing Conditions

Sample #	Date Processed	Furnace Translation Rate	Field (KG)	Comments
001AMM0	12/16/85	1 cm/min	0	Soak at 1227°C 30 min. Top ∥ to field, bottom cut ⊥.
001BMM5	12/18/85	1 cm/min	5	Soak at 1227°C 30 min. Top ∥ to field; orientation of bottom lost.
002AMM0	12/17/85	1 cm/min	0	Soak at 1227°C 40 min. Top ⊥ to "field," bottom cut ∥.
002BMM5	12/24/85	1 cm/min	5	Sample was remelted and processed after one hour soak following two failed attempts.
003AMM0	12/17/85	1 cm/min	0	Orientation lost.
003BMM5	12/23/85	1 cm/min	5	Soak at 1227°C one hour.
004BMM0	01/06/86	1 cm/min	5	Note crucible not baked out.
005AMM0	02/06/86	1 cm/min	0	Sample has large void at bottom approx. 1mm blowhole (side) all along length (~45 min. soak).
005BMM5	02/07/86	1 cm/min	5	30 min. soak. Crucible stuck in furnace during translation; broke (specimen tube shattered).
006AMM0	02/10/86	1 cm/min	0	Argon disconnected at bottle after purge. Much oxidation. 15 min. soak; bottom did not flow. Blowhole.
006BMM5	02/10/86	1 cm/min	5	Argon disconnected at bottle after purge. 15 min. soak. More "unflowed" at top than 005AMM0.
007MMC	02/13/86	1 cm/min	cycled 5/30 sec 0/60 sec	1/2 hr. purge; not disconnected; 1 hr. soak. Used 4" sample. 42mm flowed, 30 mm retained oxide skin. No holes visible.
008BMM5	02/19/86	1 cm/min	5	1 hr. purge, 1 1/2 hr. soak. Periodic bouts of vibration caused assembly to "jump."
009AMM0	07/22/86	1 cm/min	0	Magnet balking, 1/2 hr. soak, sandblasted to remove oxide.
009BMM5	07/24/86	1 cm/min	5	1/2 hr. soak; sandblasted magnet working.
010BMM5	07/24/86	1 cm/min	5	Sandblasted; 45 min. soak, magnet cut-off in last .2 cm of run.
010AMM0	07/25/86	1 cm/min	0	Sandblasted, 45 min. soak.
011BMM5	08/13/86	1 cm/min	5	Sandblasted, 30 min. soak, furnace position lower 9.0 magnet cut-off at 2.5. (<6.5 = solidification complete).
011AMM0	08/15/86	1 cm/min	0	Sandblasted, 30 min.

Stereological Measurements

Carbide Volume Fraction

A comparison of the volume fraction of carbide phase between a MAR-M 246 + Hf sample solidified under no magnetic field (Sample 003AMMO) and under a 5 KG (Sample 003BMM5) field are shown in Figure 6. Both samples exhibit carbide volume fractions of roughly 4.0%. (No field, V_V = 3.9%, 5KG, V_V = 4.15%). Results obtained for the no-field sample indicate roughly the same volume fraction down the center of the sample as along the edges. However, in the magnetic field solidified sample, the volume fraction of carbides near the edges of the sample shows some tendency to move to higher values than the center as solidification progresses. This variation does not appear to be statistically significant since subsequent samples have not shown the same trend.

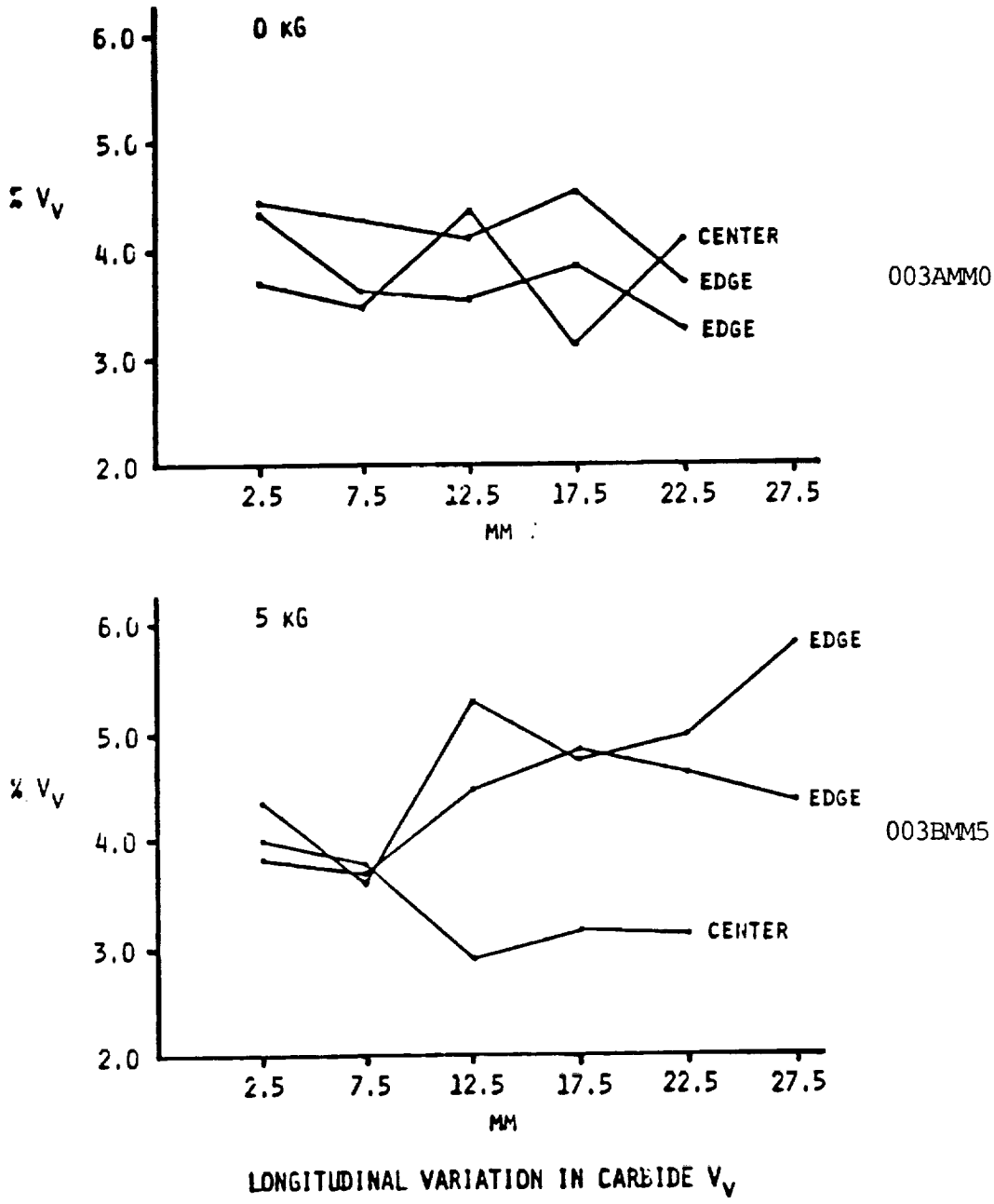

Figure 6. Comparison between the volume fraction of carbides in samples directionally solidified with no magnetic field (Sample 003AMMO) and with a 5 KG magnetic field (Sample 003BMM5). Measurements were made down the center of each sample and 2 mm in from each edge. Distances are measured from the start of solidification. Solidification rate 1 cm/min.

In general, little difference was found between the average morphological parameters of the magnetic field solidified samples and those solidified without a magnetic field. The main differences appeared to be one of uniformity, with the no-field samples being uniform while a variation was obvious between the center and edges of the field-solidified sample.

This difference may arise due to the convective damping present in the field solidified samples. Moderate convection, which is likely for the no-field samples, would tend to homogenize the liquid in advance of the solidification front. On the other hand, if convection were slowed drastically but not stopped, a slow convective roll, in conjunction with solute rejection at the interface, could lead to compositional differences between the center and edges of the sample. This could lead to radial variations in the carbide volume fraction and morphology.

Volume Fraction of the Interdendritic Eutectic

One factor which may effect the performance of a superalloy is the volume fraction of the interdendritic eutectic constituent. A detailed stereological analysis was carried out in this project in order to determine any variation in the volume fraction of the eutectic constituent with the magnetic field. The samples analysed, along with the results obtained are given in Table 2. Measurements were made until a C.V. of 5% or less was obtained. With one exception, the volume fractions of the eutectic

Table 2. Volume Fraction of the Interdendritic Eutectic Constituent

Magnetic Field Strength (KG)	Sample Number	V_v(%) - 95% C.I.	C.V.	Number of Counts
0	009AaMM0	14.65 ± 1.46	0.0495	1792
0	009AbMM0	9.55 ± 0.96	0.0498	2480
0	011AbMM0⊥	17.68 ± 1.76	0.0498	1536
5	003BMM5	17.47 ± 1.72	0.0490	1408
5	009BbMM5‖	14.45 ± 1.44	0.0497	1792
5	011BaMM5⊥	16.39 ± 1.62	0.0493	1600
5	011BbMM5⊥	14.90 ± 1.50	0.0504	1728
5	??????M5‖	15.80 ± 1.58	0.0500	1530

constituent in all samples were approximately the same. Sample 009A6MM0 which was the top half of a sample processed under no-field conditions contained a significantly lower volume fraction of the interdendritic eutectic constituents than any of the other samples. There is no obvious reason for this lower volume fraction. The lower portion of this same sample, 009AaMM0, yielded a volume fraction of 14.65% which was more in line with the results obtained in the other samples. The results obtained indicate that a 5KG transverse magnetic field had no major influence on the volume fraction of the interdendritic constituent in this study.

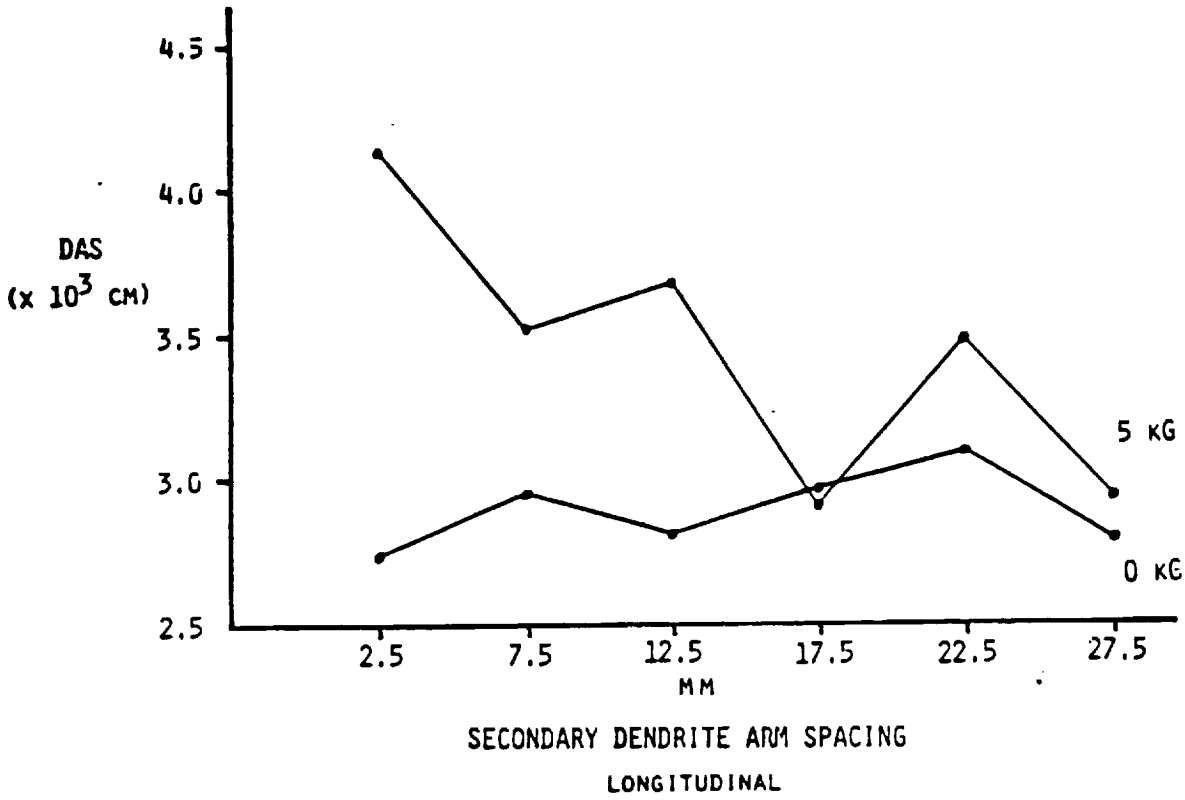

Figure 7. Secondary dendrite arm spacing as a function of amount solidified in a no-field sample 003AMMO and a 5KG solidified sample 003BMMS.

Secondary Dendrite Arm Spacing

Measurement of the secondary dendrite arm spacing as a function of distance yielded a relatively uniform spacing along the length of the no-field sample and a slight reduction in spacing with amount solidified in the 5 KG sample. These results are shown in Figure 7. The differences between the two samples cannot be considered statistically significant.

Table 3. Primary Dendrite Arm Spacing

Magnetic Field Strength (KG)	Sample Number	Primary Dendrite Spacing (mm)
0	009AbMMO	0.1303
0	011AbMMO⊥	0.1649
5	009BbMM5	0.1300
5	011BaMM5⊥	0.1576
5	011BbMM5⊥	0.1311
5	??????M5	0.1558

Primary Dendrite Arm Spacing

Transverse sections were taken of several of the samples processed in this study in order to permit measurement of the primary dendrite arm spacing. The samples analyzed and the corresponding results are given in Table 3.

From Table 3 the primary dendrite arm spacing seems to fall into two groups. One group of samples all have primary dendrite arm spacings of approximately 0.13mm. The remaining samples have primary dendrite arm spacings centered around 0.16mm. Unfortunately, there appears to be no correlation between the presence of a magnetic field and the primary dendrite arm spacing in this study. A higher field strength, different growth conditions or a different field orientation may yield different results.

Chemical Analysis

In addition to morphological changes in samples solidified under a magnetic field, it is also quite possible that compositional changes will occur. A qualitative analysis was carried out early in this project using a scanning electron microscope (SEM) and energy dispersive x-ray analysis system to roughly determine the difference in carbide compositions between a no-field (Sample 006AMMO) and a 5KG (Sample 006BMMS) solidified sample. In this analysis carbides in the upper 1 cm of the no-field and 5 KG field samples were selected at random and analyzed. Results for each sample were averaged and raw peak heights (counts) were used to compare the relative differences in composition of the carbides in the two samples. The results are shown in Figure 8. In this figure, the average counts found for a selected characteristic x-ray peak for a particular element was used as the control value. The average counts obtained from the 5 KG solidified sample were then compared to those obtained for the control. The percentage of tantalum (Ta), titanium (Ti), and tungsten (W) in the carbides were all lower in the 5 KG sample than in the no field sample, while the percentage of hafnium (Hf) was considerably higher.

It was felt that a more detailed compositional analysis was justified. During the later stages of the project two no-field MAR-M 246 + Hf samples (009AMMO, 011AMMO) and two 5 KG field samples (009BMM5, 011BMM5) were analyzed for carbide, dendrite,

CARBIDE COMPOSITION

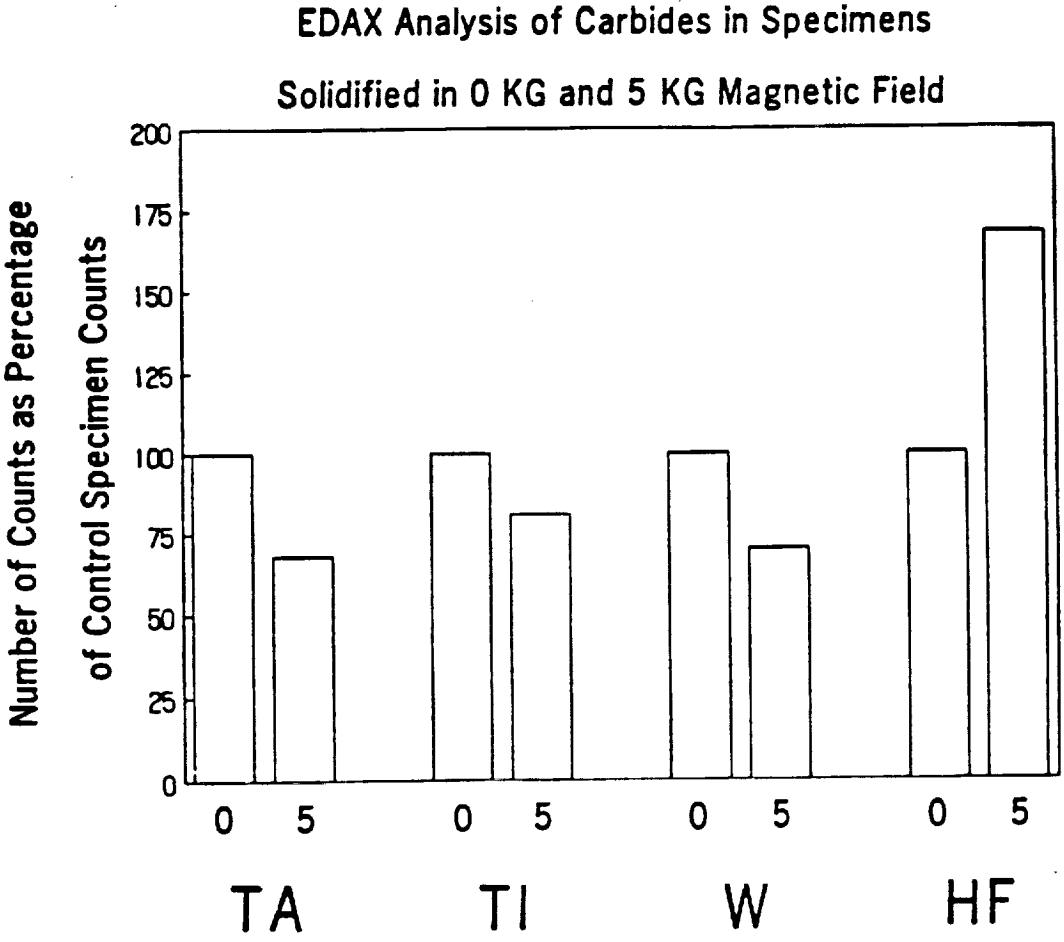

Figure 8. Comparison of carbide compositions between no-field (Sample 006AMM0) and 5KG field solidified (Sample 006BMM5) MAR-M 246 + Hf superalloys. For each element, the average characteristic x-ray peak intensity for the no-field sample was normalized to 100% to facilitate comparison with the 5 KG field sample.

interdendritic, and eutectic composition using a Cameca-SX50 microprobe and wavelength dispersive x-ray spectroscopy. Both the eutectic and dendritic regions were analyzed using the area mode. Since the interdendritic regions contained several distinct phases, these areas were analyzed using the spot mode.

Table 4. Comparison of Carbide Compositions for Field and No-Field Samples

Magnetic Field Strength (KG)	Sample Number	Element (%) Cr	Co	Ti	Al	Mo	W	Hf	Ta	Ni	Type	I.D.
0	011AaMM0⊥	2.17	1.34	13.61	0.15	7.04	28.26	11.32	30.28	5.84	2	D3
0	011AaMM0⊥	19.82	2.66	0.48	0.22	23.68	42.84	0.59	0.68	9.03	?	D4
0	011AaMM0⊥	2.55	4.39	1.98	1.41	1.47	7.51	44.21	5.96	30.56	1	D5
0	011AbMM0⊥	4.54	3.92	7.06	1.98	5.67	16.92	20.85	18.01	21.03	?	E3
0	011AbMM0⊥	3.17	6.50	0.40	0.92	0.81	0.05	38.21	1.92	48.02	1	E4
0	011AbMM0⊥	1.42	1.21	14.14	0.06	6.58	24.40	17.86	28.91	6.14	2	E5
0	009AbMM0⊥	2.18	2.58	1.52	0.88	1.02	7.87	61.06	8.41	14.47	1	A4
5 KG	009BaMM5‖	1.81	1.01	15.41	0.00	7.34	27.32	12.77	28.91	5.42	2	B4
5 KG	011BaMM5⊥	1.01	0.64	23.21	0.00	3.86	23.99	11.68	32.58	3.01	3	F3
5 KG	011BaMM5⊥	1.17	1.49	14.13	0.00	4.33	25.30	6.60	1.55	45.43	?	F4
5 KG	009BbMM5‖	1.64	0.92	27.40	0.07	4.34	20.05	13.42	23.30	8.87	3	C4
5 KG	011BbMM5⊥	1.48	0.79	36.19	0.19	2.22	16.52	14.35	24.80	3.47	3	G3
5 KG	011BbMM5⊥	2.98	2.52	11.99	0.45	6.68	25.94	12.14	24.46	12.85	2	G4

Results obtained from the microprobe analysis of the carbides in all samples are presented in Table 4. Backscattered electron images which show the actual positions analyzed in the micropobe and the sample identification numbers are included in the Appendix. The I.D. code listed for each carbide indicates the figure and spot number in the photomicrograph included in the Appendix.

While many additional carbides would have to be analyzed to establish a significant pattern, it appears that at least three types of carbides are present based on their compositions. For example, three of the thirteen carbides all have Hf levels above

approximately 40% while having Ta and W levels below 9%. These three carbides are labeled type 1 in Table 4. It is interesting that all three of these carbides were found in samples solidified with no applied magnetic field.

Another group of carbides that appear to have roughly equal compositions contain between 12 and 16% Ta, 24 to 29% W, 11 to 19% Hf, and 28 to 31% Ta. These four carbides are listed as type 2 in Table 4 and were found in both the field and no-field samples. Three of these were blocky carbides while the fourth appeared to be a script carbide plate. The fact that these carbides were found in both types of samples implies their formation is not influenced by the presence of a magnetic field.

In another grouping, three similar carbides were found which had high Ti concentrations (above 23%) combined with low Cr and Co contents (approaching 1%). These carbides are labeled as type 3 in Table 4. All three of these carbides were found in samples solidified under a magnetic field.

While these results are not statistically sound, they do indicate a possible trend with high Hf-content carbides being more likely in no-field samples and high Ti-content carbides being more likely in magnetic-field-solidified samples.

Compositional analysis was also carried out on the dendrites in both the no-field and field solidified samples. Results are presented in Table 5. From the data gathered there appears to be no appreciable difference between the composition of dendrites

Table 5. Dendrite Composition for Field and No-Field Solidified Samples

Magnetic Field Strength (KG)	Sample Number	Element % Cr	Co	Ti	Al	Mo	W	Hf	Ta	Ni	I.D. (see text)
0	011AaMM0⊥	9.42	10.64	0.86	5.85	2.03	10.40	0.35	0.95	58.51	D2
0	011AbMM0⊥	8.49	10.95	0.89	5.72	2.05	110.01	0.22	0.92	60.77	E2
0	009AbMM0	8.85	11.15	0.74	5.49	2.13	10.66	0.220	0.80	59.98	A1
5	009BaMM5‖	9.53	11.34	0.76	5.26	1.90	10.18	0.10	0.76	61.16	B1
5	011BaMM5⊥	8.34	11.12	0.80	5.53	2.07	10.84	0.25	0.76	60.29	F2
5	009BbMM5‖	8.09	10.55	0.82	5.95	2.06	10.03	0.41	0.73	61.37	C1
5	011BbMM5⊥	9.09	10.85	0.87	5.89	2.10	9.11	0.33	0.78	600.98	G2

Table 6. Composition of the Interdentritic Eutectic Constituent Field vs No-Field Samples

Magnetic Field Strength (KG)	Sample Number	Element % Cr	Co	Ti	Al	Mo	W	Hf	Ta	Ni	I.D. (see text)
0	011AaMM0⊥	8.11	8.69	1.50	6.59	2.37	5.70	4.51	1.22	61.30	D1
0	011AbMM0⊥	9.03	9.26	1.45	5.92	2.86	5.38	2.59	1.12	62.38	E1
0	009AbMM0	10.14	10.30	1.22	5.88	3.02	7.18	1.85	0.78	59.61	A2
5	009BaMM5‖	9.51	10.32	1.32	5.69	2.92	7.51	1.65	0.61	60.47	B3
5	011BaMM5⊥	9.52	9.93	1.46	6.24	3.21	6.47	2.49	0.82	59.85	F1
5	009BbMM5‖	8.87	9.87	1.30	6.27	3.28	7.89	1.64	0.89	59.99	C2
5	011BbMM5⊥	9.77	9.61	1.55	6.41	3.08	4.55	2.79	0.79	61.45	G1

formed during solidification under no-field conditions and those formed during solidification under a 5 KG field.

The interdendritic eutectic constituent was also analyzed using wavelength dispersive x-ray spectroscopy on the microprobe. The results obtained are presented in Table 6. Again, no apparent differences were found in the compositions of the eutectic constituent between the no-field and 5 KG field solidified samples.

Solidification Under Cyclic Field Conditions

One Sample (007MMC) was processed in which the magnetic field was applied intermittently in order to mimic the low-g, high-g periods of solidification obtained in experiments performed on NASA's KC-135 zero-g aircraft. Since both a magnetic field and microgravity conditions serve to reduce fluid flow during solidification, it is often assumed that solidification under a magnetic field will produce structures very similar to those obtained during solidification under microgravity conditions. While this may be justified as a first approximation, there are important differences between the influence of these two conditions on the solidification process.

A steady magnetic field during solidification slows all fluid movement. This includes damping of gravity driven flows, surface tension driven flows and any other flows. The situation is different in the case of microgravity solidification. Here the driving force for normal convection and sedimentation is removed. However, it is important to note that fluid movement is not restricted. Indeed it has been stated that flows of only minor importance under 1-g conditions, such as as surface tension induced flows, may become dominate factors during solidification under microgravity conditions.

While in depth, long duration microgravity studies must be carried out in order to gain a true understanding of the significance of these various flows on the solidification process

and the resulting microstructural features, some insight can be gained from a simple comparison of structures obtained from experiments performed on the KC-135 and experiments carried out using intermittent applications of a magnetic field. In KC-135 directional solidification studies on MAR-M 246+Hf alloys performed by Johnston et al.[1], samples were solidified during repetitive exposure to approximately 30 seconds of low gravity followed by approximately 45 seconds of high gravity (up to 1.8g). This was carried out for several cycles. Johnston's results indicated a variation in the volume fraction of the carbide phase as shown in Figure 9.

For comparison purposes, in the current study samples were solidified while being subjected to a repetitive exposure of 30 seconds of applied field followed by 60 seconds of no field. While this will not completely duplicate the environment experienced in the KC-135, the results at least provide some means of distinguishing between the influence of a magnetic field and the influence of low-gravity conditions on the solidification process. It must be remembered in the interpretation of these structures that steady state conditions are probably not reached and that comparisons are actually being made between transient structures.

MAR-M 246+Hf samples were directionally solidified at a rate of 1 cm/minute and the magnetic field turned on for 30 seconds at 5000 Gauss, then off for 60 seconds. This was repeated throughout solidification. The magnetic field was oriented horizontally and a vertical growth direction was utilized. The sample was sectioned

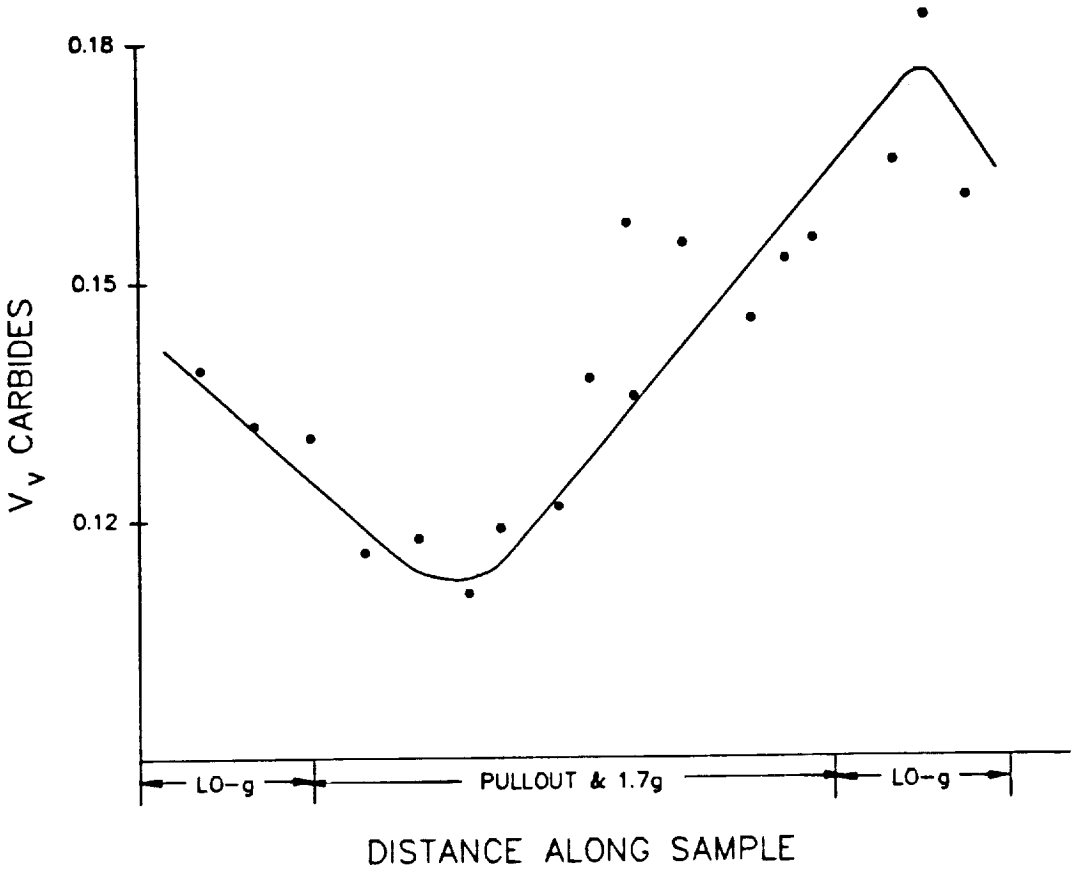

Figure 9. Variation of carbide volume fraction with gravity level in a KC-135 solidified sample.

longitudinally, mounted, and prepared using standard metallographic procedures. A one cm long section of the unetched sample was thoroughly analyzed in order to cover one full cycle of the magnetic field.

Volume fraction (V_v), number per unit length (N_L), and the number per unit area (N_A) of the carbide phase were measured in order to permit determination of the shape factor if desired. Since the experiment was cyclic, measurements were taken every 0.25 mm vertically and horizontally to observe both vertical variations

Table 7. Carbide Volume Fraction (V_v) and Coefficients of Variation for Intermittent Field Sample

Vert. Distance-mm	Left %	C.V.	Center %	C.V.	Right %	C.V.
2.5	4.2	1.3	4.0	1.5	5.1	0.9
5.0	2.1	3.1	3.3	0.9	4.3	1.2
7.5	1.9	3.9	3.8	1.7	4.5	1.2
10.0	1.9	1.8	2.8	1.6	3.7	1.4

and variations across the sample. Shape factors were then calculated at positions of 2.5 mm, 5.0 mm, 7.5 mm, and 10.0 mm from the starting position and were carried out for locations at the left, center and right of the sample. A range of values of 0.75 mm above, below and around each interval point was incorporated into the statistical results with placements made at every 0.25mm.

The results of the carbide volume fraction, V_v, number per unit length, N_L, and number per unit area, N_A, calculations are tabulated in Tables 7, 8 and 9. In addition, a graph of the carbide volume fraction as a function of position on the sample is shown in Figure 10. As noted in Tables 7, 8 and 9 the coefficients of variation for each measurement are quite large as compared to a more desirable value of 0.05. The large values result due to globules of the carbides in the matrix. Even over the small range of 0.75 mm, the data points varied widely. From statistical

Table 8. Carbide Number Per Unit Length (N_L) and Coefficients of Variation for Intermittent Field Sample

Vert. Distance-mm	Left(mm^{-1})	C.V.	Center(mm^{-1})	C.V.	Right(mm^{-1})	C.V.
2.5	17.28	0.1	17.89	0.1	17.67	0.2
5.0	17.82	0.1	16.90	0.1	19.00	0.2
7.5	15.21	0.1	14.90	0.2	15.70	0.2
10.0	14.29	0.1	17.00	0.1	16.20	0.1

Table 9. Carbide Number Per Unit Area (N_A) and Coefficients of Variation for Intermittent Field Sample

Vert. Distance-mm	Left(mm^{-2})	C.V.	Center(mm^{-2})	C.V.	Right(mm^{-2})	C.V.
2.5	1.65 x 10	0.2	2.08 x 10	0.1	1.93 x 10	0.1
5.0	1.65 x 10		1.86 x 10		2.17 x 10	
7.5	1.92 x 10		2.41 x 10		1.93 x 10	
10.0	1.57 x 10		1.84 x 10		2.02 x 10	

calculations, 500 to 1000 counts would be necessary to obtain a coefficient of variation of 0.05 for each value of V_v, N_L, and N_A measured. This was obviously impossible due to the limited area over which counts could be taken.

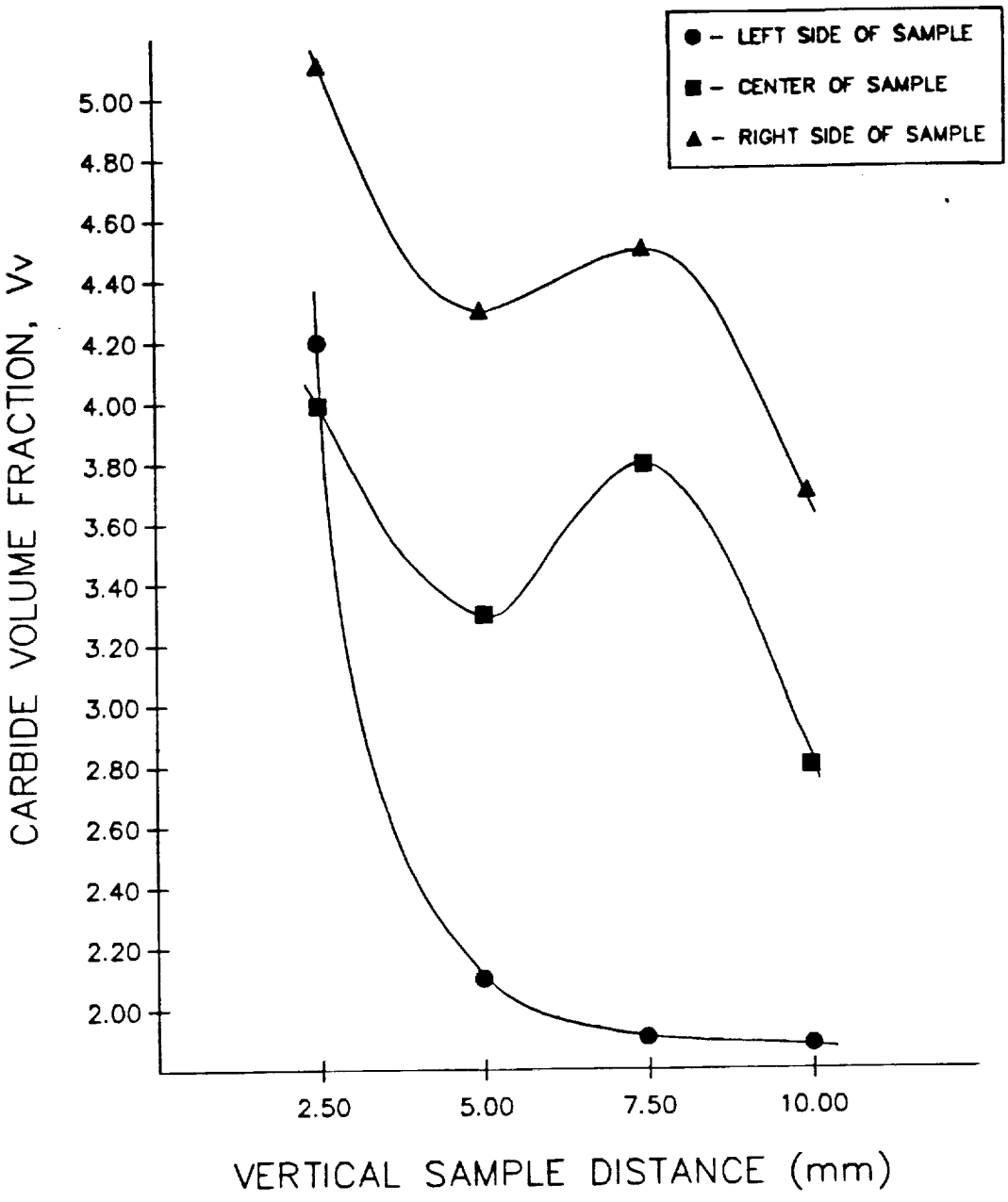

Figure 10. Variation of carbide volume fraction with position on a sample solidified under intermittent magnetic field conditions.

The variation in volume fraction of the carbide phase which resulted due to the cyclic magnetic field should be compared to the results obtained on KC-135 solidified samples as shown in Figure 10. In an attempt to characterize the carbides by shape, the V_v,

TABLE 10. CARBIDE SHAPE FACTORS FOR INTERMITTENT FIELD SAMPLE

Vertical Distance	Left	Center	Right
2.5	0.91	0.82	0.67
5.0	1.94	0.99	0.82
7.5	1.36	0.51	0.60
10.0	1.45	1.22	0.75

N_L, and $N_A$values were used to determine the shape factor, F_1, as described by Fishmeister.[19] This shape factor is given by

$$F_1 = (2/3\pi) \cdot (N_L^2/V_V N_A)$$

and has a value of one for spherical particles and increases with increasing complexity of shape. Results are tabulated in Table 10 and are plotted in Figure 11.

Referring to Figure 11, it is apparent that as the vertical distance along the sample increases, the shape factors cycle. This cyclic pattern should indicate that the carbide morphology changes with position. However, the shape factor was expected to cycle in such a way that it approached a small value close to one for the blocky carbides and increased to a higher value as more script carbides formed. The fact that values considerideriably less than one were obtained for F_1 are questionable. In addition, the variations observed appear to be primarily due to changes in the volume fraction of the carbide phase. As discussed previously,

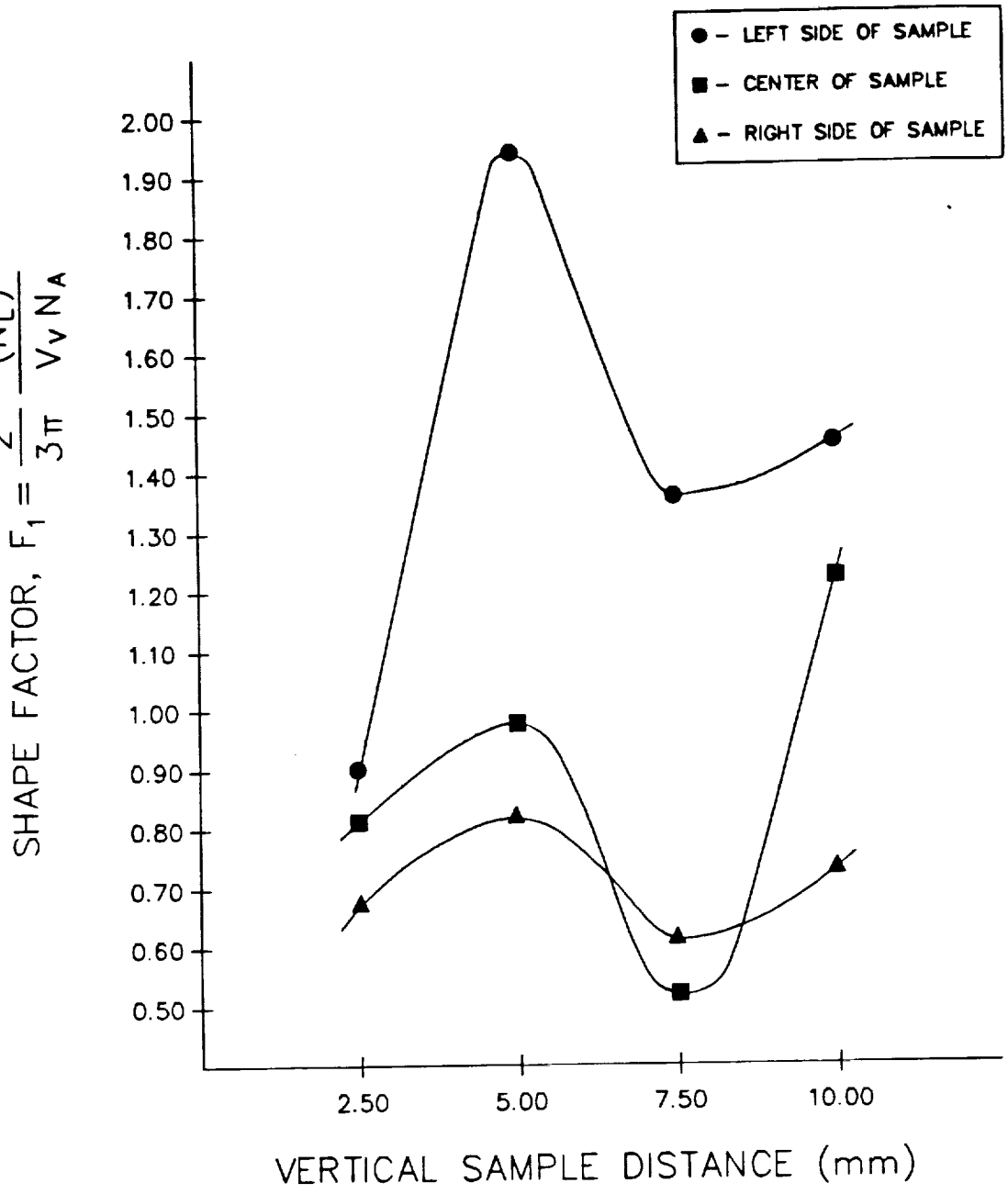

Figure 11. Variation in the shape factor, F_1, of carbide particles vs position for a sample solidified under intermittent magnetic field conditions.

this shape factor does not appear to be an appropriate indication of carbide particle shape for this investigation.

The cycling effect of the volume fraction of the carbide phase could be explained by a dependence on the composition of the solidifying liquid. In the absence of a magnetic field, when solute is rejected into the liquid at the solid-liquid interface it can be distributed by convective fluid flow resulting in a fairly uniform composition across the sample. However, when a magnetic field is applied to the system, the convective fluid flow is damped. This results in a slower distribution of the rejected solute in the liquid and an effective change in the solute field adjacent to the interface. It's quite conceivable these changes will result in modification of the volume fraction of carbides formed.

The results of this analysis indicate that a variation in the volume fraction of the carbide phase does occur when a magnetic field is varied during directional solidification of MAR-M 246+Hf alloys. However, dependence of the volume fraction of carbide on the magnetic field should be investigated further. Microprobe analysis should have been carried out to specifically investigate the compositional variation across the sample. Unfortunately, with several project directors, the necessary transfer of files and other project materials has apparently resulted in this particular sample (007MMC) being misplaced. Further analysis is not possible. It should be pointed out that different conclusions may be reached upon comparison of steady state magnetic field structures with structures obtained from longer term microgravity solidification studies carried out on the orbiter.

CONCLUSIONS

This project was designed to provide an analysis of the effects of magnetic fields on microstructural features in directionally solidified dendritic superalloys, with special reference to the influence on carbide morphology. It was hoped that script vs blocky carbide shapes could be distinguished using a shape parameter. However, the inability to determine N_V values from N_A measurements on a plane section through a convoluted particle makes this approach inadequate. The nature of this problem is such that an accurate characterization of script vs blocky carbides may require the use of a three-dimensional technique.

Serial sectioning would provide the best information on the extent of carbide networking in script morphologies as opposed to blocky. However, it may not be necessary to fully characterize carbide shape in order to investigate the effect of shape on material properties. It has been shown that properties in the cast iron system are linearly related to graphite S_v values, and the same may prove true for carbides in superalloys.

Furthermore, there are other approaches which provide useful information toward crack propagation predictions. Curvature measurements, which would give an indication of the degree of "sharpness" at carbide edges, could be performed in two dimensions. If evidence is found that cracks are propagated into the matrix at sharp carbide edges, then this measurement may yield significant

information without resorting to a three-dimensional analysis.

The main thrust in this study was to determine the influence of a magnetic field on the microstructures obtained in directionally solidified Mar-M 246 + Hf. A steady magnetic field of 5KG oriented transverse to the vertical growth direction appeared to have little influence on the carbide volume fraction, primary dendrite arm spacing and secondary dendrite arm spacing of a sample directionally solidified at 1 cm/mm. However, it was noted that samples solidified without a magnetic field appeared to have a more uniform structure radially than those solidified with a field. Coorelations could not be made between the volume fraction of the interdentric eutectic constituent and the presence of a magnetic field during solidification.

Chemical analysis indicated some differences between the compositions of carbides formed during solidification with a magnetic field and those formed without a field. It is conceivable that a variation in carbide morphology could result due to these compositional variations and could be used to advantage. No significant trends were found in the variation of the composition of the dendrites or of the interdendritic constituent with a magnetic field.

The most dramatic variations in microstructure were observed in a sample processed under cycled magnetic field conditions. Here, changes in the volume fraction and shape factor were found to occur as the field was cycled. While measurable variations were observed, it must be remembered that the statistics of this portion

of the analysis are relatively poor due to a limited sampling area. In addition, it is unlikely that steady state conditions were ever reached during processing.

While the above study was comprehensive within its constraints, additional work is considered desirable in order to gain a more complete understanding of the possible influences of magnetic fields on the solidification process. Higher magnetic field strengths and difficult orientations may have significant effects on the solidification process and the structures obtained. Future work should be carried out to investigate the influence of these variables.

ACKNOWLEDGEMENTS

The Principal Investigator would like to acknowledge the help of Ms. Wendy Alter and Ms. Allison Sandlin who carried out much of the sample preparation and quantitative metallographic analysis reported in this study. Special thanks are due Ms. Dianne Schmidt who has unselfishly participated in gathering and analyzing data during the past few months. Completion of this project would not have been possible without her help. Thanks are also due to Mr. Steve Gentz whose comments, suggestions and assistance have played a major role in meeting the science goals of this project. I would also like to thank Dr. Mary Hellen McKay and the Marshall Space Flight Center who thought this work was of sufficient interest to provide funding for the project.

REFERENCES

1. M. H. Johnston and P. A. Curreri, Personal Communication (1984).

2. Metals Handbook, Desk Edition, American Society for Metals, Metals Park, Ohio (1984).

3. R. J. Naumann, "Microgravity Science and Applications Program Description Document," NASA, Space Science Laboratory (1984).

4. H. P. Utech, M. C.Flemings, "Thermal Convection in Metal-Crystal Growth: Effect of a Magnetic Field," Supplement to Journal of Physics, Chem. of Solids, p. 651-658 (1966).

5. M. C. Flemings, Solidification Processing, McGraw Hill, Inc., New York, New York (1974).

6. Metals Handbook, Ninth Edition, Volume 3, Properties and Selection: Stainless Steels, Tool Materials and Special-Purpose Metals, American Society for Metals, Metals Park, Ohio (1980).

7. S. R. Coriell, M. R. Cordes, W. J. Boettinger, R. F. Sekerka, "Convective and Interfacial Instabilities During Unidirectional Solidificaiton of a Binary Alloy," J. of Crystal Growth, Vol. 49, p. 13-28 (1980).

8. T. G. Cowling, Magnetohydrodynamics, Interscience Publishers, Inc., New York, New York (1957).

9. S. Chandrasekhar, Hydrodynamic and Hydromagnetic Stability, Oxford University Press, London (1961).

10. H. P. Utech, M. C. Flemings, "Elimination of Solute Banding in Indium Antimonide Crystals by Growth in a Magnetic Field," J. of Applied Physics, Vol. 37, No. 5, p. 2021-2024 (1966).

11. H. A. Chedzey, D. T. J. Hurle, "Avoidance of Growth-Striae in Semiconductor and Metal CrystalsGrown by Zone-Melting Techniques," Nature, Vol. 210, p. 933-934 (1966).

12. H. P. Utech, W. S. Brower, J. G. Early, "Thermal Convection and Crystal Growth in Horizontal Boats: Flow Pattern, Velocity Measurement, and Solute Distribution," Supplement to J. of Physics, Chem. of Solids, p. 201-205 (1966).

13. S. Sanghamitra, W. R.Wilcox, "Non-Constant Distribution Coefficients for Directionally Solidified InSb-GaSb," Mat. Res. Bull., Vol. 13, p. 293-302 (1978).

14. P. R. Sahm, "Modified Microstructure in Eutectic Au-Co Alloys by Use of a Magnetic Field During Directional Solidification," J. of Crystal Growth, Vol. 6, p. 101-103 (1969).

15. P. R. Sahm, H. R. Killias, "Directional Solidification of Eutectic and Off-Eutectic Au-Co Composites With and Without Magnetic Field," J. Mat. Sci., Vol. 5, No. 12, p. 1027-1037 (1970).

16. J. D. Verhoeven, D. D. Pearson, "The Effect of a Magnetic Field Upon Directional Solidification of Sn-Cd and Sn-Pb Alloys," J. of Mat. Sci., Vol. 8, p. 1409-1412 (1973).

17. Y. Aoki, S. Hayashi, H. Komatsu, "Directional Solidification of Aluminum-Silicon Eutectic Alloy in a Magnetic Field," J. of Crystal Growth, Vol. 62, p. 207-209 (1983).

18. E. E. Underwood, Quantitative Stereology, Addison-Wesley Publishing Co., Reading, Massachusetts (1970).

19. H. F. Fischmeister, "Shape Factors in Quantitative Microscopy," Z. Metalikde, Vol. 65, p. 558-562 (1974).

APPENDIX - Microprobe Analysis Areas

Backscattered electron images of areas analyzed using the Cameco SX50 microprobe and wavelength dispersive x-ray spectroscopy are shown on the following pages.

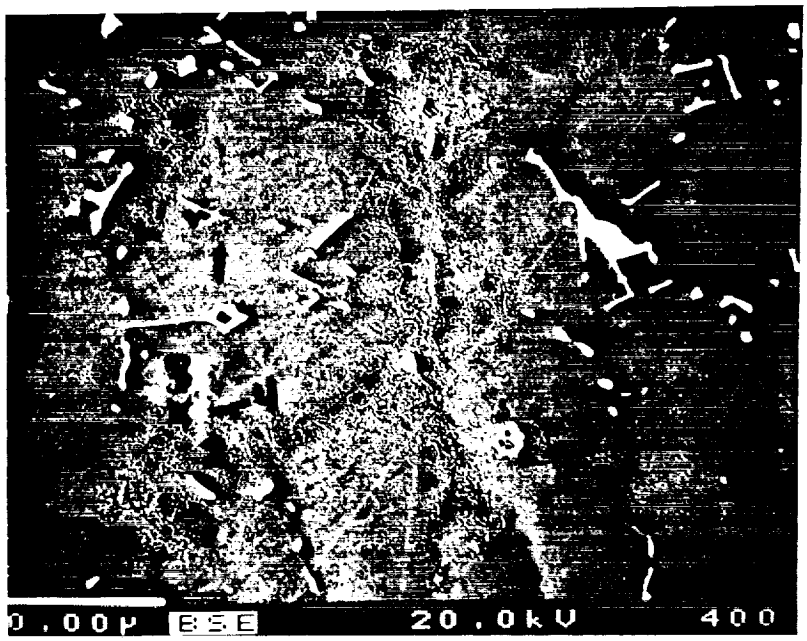

Figure A. Photomicrograph of a MAR-M 246 + Hf sample directionally solidified at 1 cm/min without a magnetic field. Sample 009AbMMO. Photo was taken from the upper portion of the sample (i.e., last to solidify). Backscattered electron image.

Figure B. Photomicrograph of a MAR-M 246 + Hf sample solidified at 1 cm/min under a 5 K Gauss magnetic field. Sample 009BaMM5. Sample was sectioned parallel to the field direction. Photo is from lower portion of sample (i.e., first to solidify).

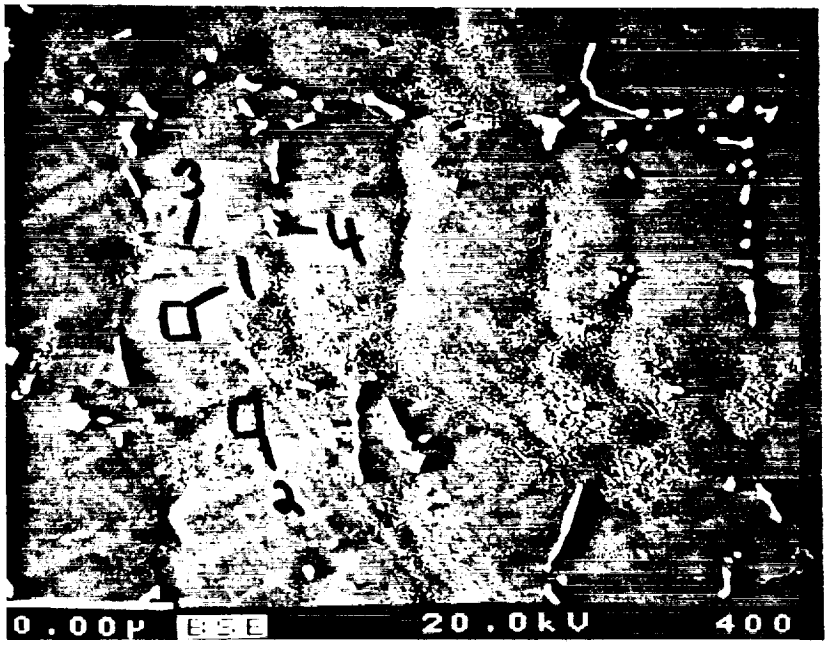

Figure C. Photomicrograph of a MAR-M 246 + Hf sample directional solidified at 1 cm/min under a 5 K Gauss magnetic field (Sample 009BbMM5). Sample was sectioned parallel to the field direction. Photo was taken from top half of sample shown in Fig. B. Backscattered electron image.

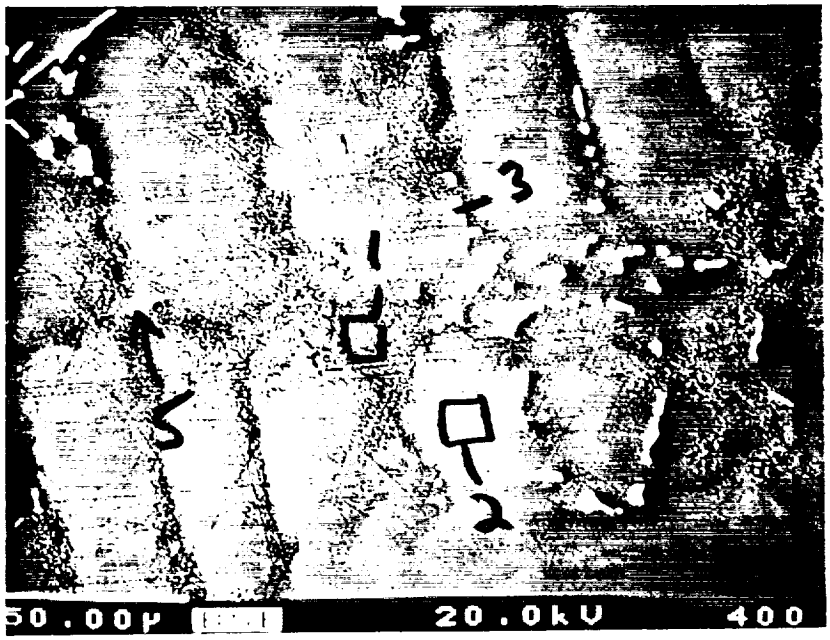

Figure D. Photomicrograph of a MAR-M 246 + Hf sample directionally solidified at 1 cm/sec under no magnetic field (Sample 011AaMM0). Photo is from the lower half of the sample.

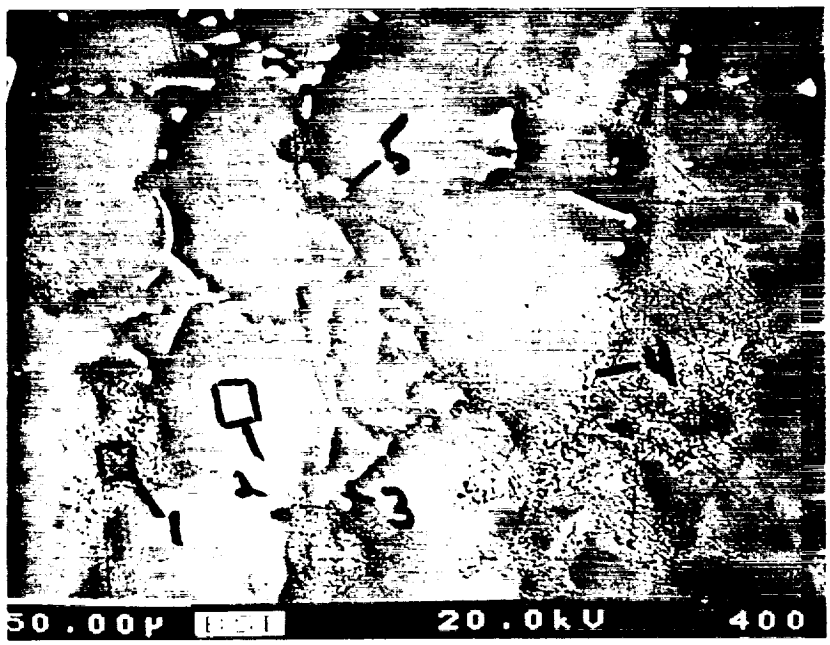

Figure E. Photomicrograph of a MAR-M 246 + Hf sample directionally solidified at 1 cm/min with no magnetic field (Sample 011AbMM0). Photo is from the upper half of the sample in Figure D. Backscattered electron image.

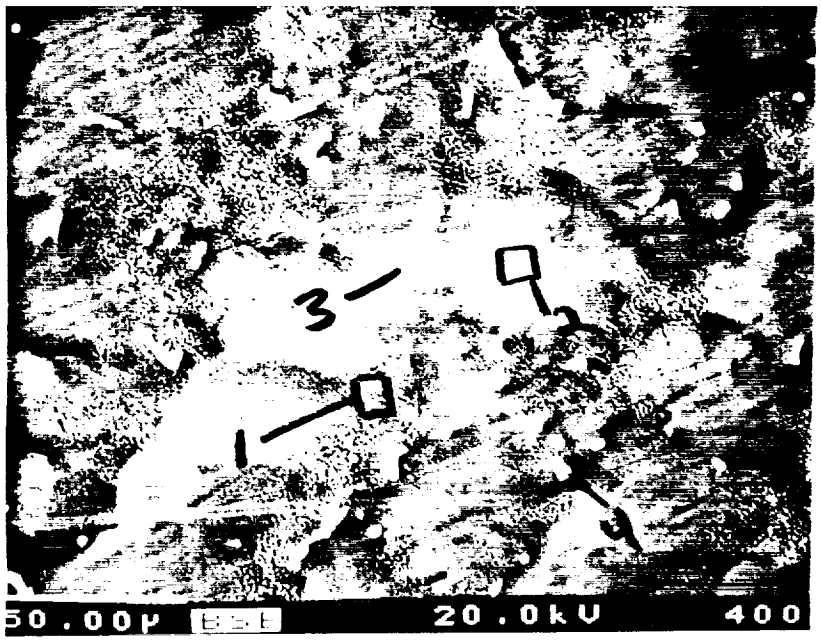

Figure F. Photomicrograph of a MAR-M 246 + Hf sample directionally solidified at 1 cm/min under a 5 K Gauss magnetic field (Sample 011BaMM5). Sample was sectioned perpendicular to the field orientation. Photomicrograph is from lower portion of the sample. Backscattered electron image.

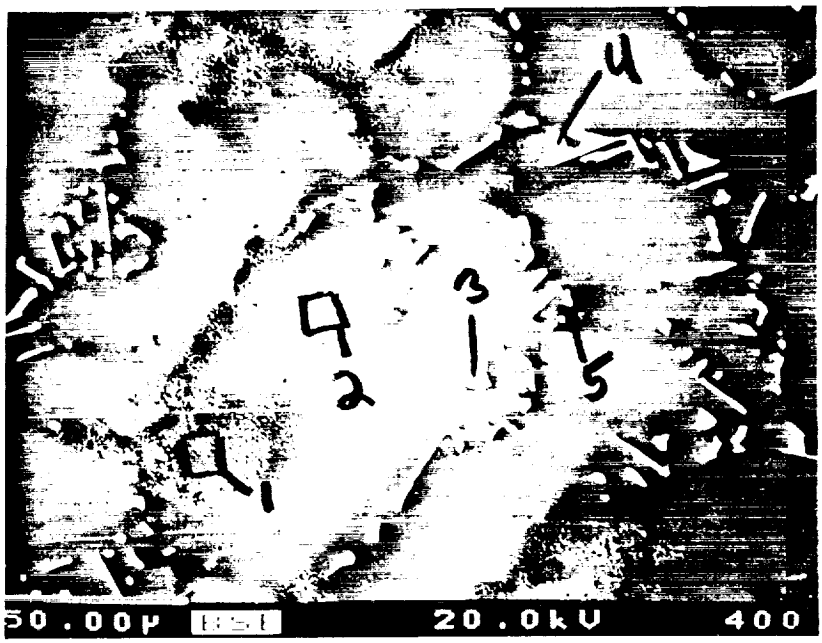

Figure G. Photomicrograph of a MAR-M 246 + Hf sample directionally solidified at 1 cm/min under a 5 K Gauss magnetic field (Sample 011BbMM5). Sample was sectioned perpendicular to the field orientation. Photo micrograph is from upper portion of sample in Figure F. Backscattered electron image.